

Stoichiometry and volume dependent transport in lithium ion memristive devices

Charis M. Orfanidou, Panagiotis S. Ioannou, Evripides Kyriakides, Christiana Nicolaou, Cristian N. Mihailescu, Van Son Nguyen, Van Huy Mai, Olivier Schneegans, and John Giapintzakis

Citation: *AIP Advances* **8**, 115211 (2018); doi: 10.1063/1.5051568

View online: <https://doi.org/10.1063/1.5051568>

View Table of Contents: <http://aip.scitation.org/toc/adv/8/11>

Published by the [American Institute of Physics](#)

Articles you may be interested in

[Origin of negative resistance in anion migration controlled resistive memory](#)

Applied Physics Letters **112**, 133108 (2018); 10.1063/1.5021019

[Perspective: A review on memristive hardware for neuromorphic computation](#)

Journal of Applied Physics **124**, 151903 (2018); 10.1063/1.5037835

[Performance enhancement of TaO_x resistive switching memory using graded oxygen content](#)

Applied Physics Letters **113**, 183501 (2018); 10.1063/1.5048098

[Electric field modulated ferromagnetism in ZnO films deposited at room temperature](#)

Applied Physics Letters **112**, 162408 (2018); 10.1063/1.5022597

[Conduction mechanisms at distinct resistive levels of Pt/TiO_{2-x}/Pt memristors](#)

Applied Physics Letters **113**, 143503 (2018); 10.1063/1.5040936

[Light-controlled stateful logic operations using optoelectronic switches based on p-Si/HfO₂ heterostructures](#)

Applied Physics Letters **112**, 063503 (2018); 10.1063/1.5018226



Don't let your writing
keep you from getting
published!

AIP | Author Services

Learn more today!

Stoichiometry and volume dependent transport in lithium ion memristive devices

Charis M. Orfanidou,¹ Panagiotis S. Ioannou,¹ Evripides Kyriakides,¹ Christiana Nicolaou,¹ Cristian N. Mihailescu,^{1,2} Van Son Nguyen,³ Van Huy Mai,⁴ Olivier Schneegans,⁵ and John Giapintzakis^{1,a}

¹Department of Mechanical and Manufacturing Engineering, University of Cyprus, 75 Kallipoleos Avenue, P.O. Box 20537, 1678 Nicosia, Cyprus

²National Institute for Laser, Plasma and Radiation Physics, 409 Atomistilor Street, P.O. Box MG-36, 077125 Magurele, Romania

³Solar Technologies Department, Heterojunction Solar Cells Laboratory, Commissariat à l'Énergie Atomique et aux Énergies Alternatives, 50 Avenue du Lac Léman, 73375 Le Bourget-du-Lac, France

⁴Department of Optical Electronic Devices, Le Quy Don Technical University, 236 Hoang Quoc Viet, Hanoi, Vietnam

⁵Laboratoire de Génie Électrique et Électronique de Paris, CNRS, UPMC and Paris-Sud Universities, Centralesupélec, 11 rue Joliot-Curie, 91192 Gif-sur-Yvette, France

(Received 10 August 2018; accepted 5 November 2018; published online 13 November 2018)

Li_xCoO_2 , a thoroughly studied cathode material used extensively in Li-ion rechargeable batteries, has recently been proposed as a potential candidate for resistive random access memory and neuromorphic system applications. Memristive cells based on Li_xCoO_2 thin films have been grown on Si substrates and two-probe current-voltage measurements were employed to investigate the origin and nature of resistive switching behavior exhibited by these cells. The results indicate that a voltage-driven metal-to-insulator transition of the active Li_xCoO_2 layer is responsible for the resistive switching behavior, which has a homogeneous nature. © 2018 Author(s). All article content, except where otherwise noted, is licensed under a Creative Commons Attribution (CC BY) license (<http://creativecommons.org/licenses/by/4.0/>). <https://doi.org/10.1063/1.5051568>

Resistive switching (RS) in metal-insulator-metal (MIM) structures was originally reported in the 1960s¹ and has attracted the renewed interest of the information materials and devices community during the last decade.^{2–7} The potential applications of RS extend from non-volatile resistive random access memory (ReRAM) to memristor-based logic devices and neuromorphic computing systems.⁸ Identification of the RS mechanism in the proposed memristive cells - which also behave as nanobatteries⁹ - is the final obstacle that researchers need to overcome in order to transition from “lab” to “fab” manufacturing.^{3–5}

RS structures have been extensively studied and a filamentary switching mechanism has been safely established for the vast majority of implementations.^{2–7} However, the filamentary mechanism occasionally implies an electroforming step prior to operation. Furthermore, the downscaling potential of filamentary RS devices may be limited by the filament size.¹⁰ Although research efforts are mainly focused on the deeper understanding of the filamentary RS mechanism, identifying materials where a bulk mechanism is responsible for RS, in addition to being compatible with the current integrated circuit technology, can also be of high research interest. Taking advantage of recent advancements in Li integration into current CMOS processes,¹¹ an emergent structure belonging to this category is the Li_xCoO_2 -based RS device.^{12,13} A typical cell of this type consists of a Li_xCoO_2 thin film, as the active constituent layer, grown on a doped Si substrate covered with an ultrathin layer of native SiO_2 , and a Au top electrode. In such a configuration, it has already been observed that Li ions

^aAuthor to whom correspondence should be addressed: giapintz@ucy.ac.cy

are involved in the RS;¹⁴ however, the relation of Li stoichiometry to the RS mechanism remains unanswered. A second important question concerns the nature (filamentary/homogeneous) of the RS. Hence in this work, Au/Li_xCoO₂/SiO₂/Si cells have been investigated using conventional two-probe current-voltage measurements, with the aim of understanding the origin and nature of the mechanism that governs RS phenomena in these cells.

Li_xCoO₂ thin films were deposited on highly doped p⁺⁺-type Si (111) wafers by RF magnetron reactive sputtering (Alcatel SCM 600 apparatus) using a stoichiometric LiCoO₂ target, with an applied RF power of 500 W. The films were grown at room temperature in a 3:1 Ar/O₂ (process pressure 2.2 Pa) atmosphere and a bias of 250 V was applied to the substrate. The films were measured using cross-section transmission electron microscopy (TEM) and determined to have a thickness of 100 nm. They were subsequently annealed at 580 °C for 1 h in air in order to obtain the R-3m high-temperature Li_xCoO₂ phase. The crystallinity and phase purity of the Li_xCoO₂ films were investigated by GIXRD and measurements were carried out using a 9 kW rotating anode Rigaku SmartLab X-ray diffractometer. TEM studies have shown that the particular annealing step increases the native SiO₂ layer thickness from ~2-3 nm to ~8-9 nm.¹³ After completing the Li_xCoO₂ film characterization, DC-sputtered 100 nm-thick Au electrodes were deposited on top of the films through shadow masks with square apertures (sizes of: 500x500, 400x400, 300x300, 200x200, 100x100 μm²).

The room-temperature current-voltage (I-V) characteristics of all cells were measured in air ambience using a two-probe setup (Keithley 6487) sourcing voltage and measuring current. 20 μm-radius Be-Cu tips, controlled using micro-manipulators, were used to make contact with the top (Au) and bottom (Si) electrodes. The bottom electrode was in contact with the tip via a Cu block on which the sample was attached with Ag paste. The measurements were carried out by voltage sweeping and a single protocol was used for all the results presented herein. Voltage sweeps (0 V → -5 V → +5 V → 0 V, with 0.1 V step) took place with a current limit of 25 mA imposed by the instrument. In addition to the experimental studies, simulation studies were performed using COMSOL Multiphysics®.

Chemical delithiation experiments of Li_xCoO₂ films were carried out in K₂S₂O₈ aqueous solutions (25 mg/ml).¹⁵ Temporally regulated infusions of the thin film devices in the acidic aqueous solution under moderate agitation and at 50 °C were carried out. Three successive delithiation infusions, followed by deionized water rinsing, drying under N₂ stream, and GIXRD measurements of the (003) peak shift enabled the time-dependent observation of Li⁺ diffusion from the film to the acidic solution. The total delithiation process time was 1 hour and 45 minutes.

All Li_xCoO₂ films were polycrystalline and partially textured. Grazing incidence X-ray diffraction (GIXRD) patterns exhibited two relatively strong Bragg reflections that correspond to the (003) and (101) planes of the high-temperature (HT) phase of LiCoO₂. Taking into account that there is no epitaxy and thus no strain effects, the calculated value of the c-axis lattice parameter corresponds to Li content $x \sim 1$ based on the empirical relationship between x and c-axis lattice parameter length for bulk materials.¹⁶ Therefore, the annealed sputtered-grown Li_xCoO₂ films are in the insulating phase.

Fig. 1 depicts a typical J-V hysteresis loop of an Au/Li_xCoO₂/SiO₂/Si cell indicating RS behavior, with the highly coherent cycling endurance demonstrated in the inset. For this type of cell to exhibit RS behavior, it is necessary to start the cycle by applying a negative bias voltage to the Si bottom electrode. The observed RS behavior is of bipolar type, i.e., the SET process (switching from high resistive state (HRS), to low resistive state (LRS); ON) occurs for a negative bias voltage while the RESET process (switching from LRS to HRS; OFF) occurs for a positive bias voltage (resistance ratio $R_{HRS}/R_{LRS} = 71$).

RS behavior has already been observed in memristive cells based on Li_xCoO₂ thin films grown by RF-sputtering.^{12,13} The proposed mechanism responsible for the RS behavior of the investigated Au/Li_xCoO₂/SiO₂/Si memristive cells involves voltage-driven diffusion of Li ions.¹³ Specifically, it has been proposed that the electrochemical redox reactions that take place under the application of the bias voltage result in the intercalation/deintercalation of Li⁺ ions to/from the Li_xCoO₂ thin film and hence, in the occurrence of a reversible metal-to-insulator transition of Li_xCoO₂ layer. This mechanism is akin to the stages of charging and discharging of Li-ion rechargeable batteries. This is most prominently evident in the abrupt changes observed in the J-V curves of Fig. 1. These sharp transitions are associated with the dissociation energy of Li⁺ in Li_xCoO₂ (~3.95 V¹⁷⁻¹⁹)

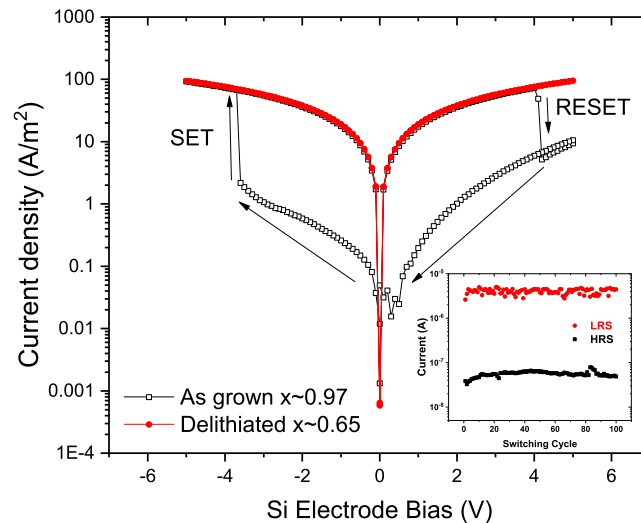


FIG. 1. Voltage sweeps before ($x \sim 0.97$, black open squares) and after ($x \sim 0.65$, red filled circles) chemical delithiation of a Au/Li_xCoO₂/SiO₂/Si memristive cell (I-V sweeps were performed on 500x500 μm^2 Au electrodes). Inset shows LRS and HRS distribution over 100 RS cycles.

which manifests – with sufficiently high sweep rates – into an abrupt change in current. Moreover, it is noted that the contribution of oxygen vacancies to RS has not been considered in this study because there has been no experimental evidence for the presence of oxygen vacancies in Li_xCoO₂²⁰ and this has been recently attributed to their high formation energy based on density functional calculations.²¹

The temporal breakdown of this reversible process (i.e. the intercalation/deintercalation of Li⁺ ions to/from the Li_xCoO₂ thin film) is as follows: The cells are fabricated in the battery-equivalent discharged state, in which Li⁺ ions are located between the CoO₂ block layers (Fig. 2(a)). Therefore, Li_xCoO₂ is in its insulating phase, where Li content is $0.95 < x < 1$,¹⁶ and the cell is in HRS. Upon the action of a negative bias voltage to the Si electrode, Li⁺ ions deintercalate from the Li_xCoO₂ cathode; concurrently, the valence state of Co ions shifts from 3+ to 4+ (oxidation) and electrons from 3+ to 4+ (oxidation) are released to the external circuit. The deintercalated Li⁺ ions are transported through the SiO₂ layer to the negatively charged Si anode¹⁴ and upon reaching the SiO₂/Si interface are reduced to neutral Li atoms, which chemically react with the Si atoms to form Li-Si compounds.²² This is equivalent to the charging process of a battery and, due to Li⁺ deintercalation, Li_xCoO₂ is expected to transform to a metallic phase, switching the cell to LRS (Fig. 2(b)). Therefore, the SET process in this memristive cell parallels the charging process of a Li-ion battery cell. Upon the application of a positive bias voltage to the Si electrode, the reverse mechanism occurs, which is the battery-equivalent discharging process and, due to Li⁺ intercalation, Li_xCoO₂ is expected to transform to an insulating

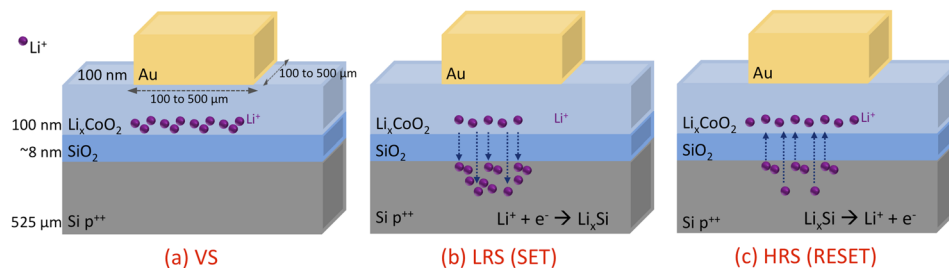


FIG. 2. Schematic view of a Au/Li_xCoO₂/SiO₂/Si memristive cell and the mechanism proposed: (a) cell at virgin state (VS), (b) cell at LRS, and (c) at HRS.

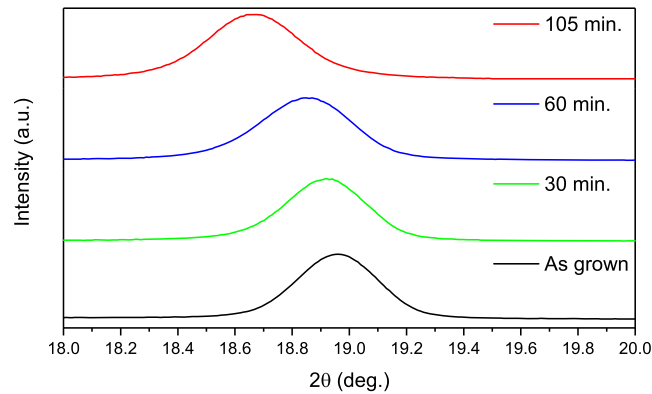


FIG. 3. GIXRD patterns showing the shift of the (003) Li_xCoO_2 peak after repeated delithiation steps, indicating a reduction of the Li content (incidence angle is 1°).

phase, switching the cell back to HRS (Fig. 2(c)). Therefore, the RESET process in this memristive cell parallels the discharging process of a Li-ion battery cell.

In order to validate that Li-ion intercalation/deintercalation – and the consequent reversible metal-to-insulator transition of the Li_xCoO_2 layer – is responsible for the observed RS behavior of $\text{Au}/\text{Li}_x\text{CoO}_2/\text{SiO}_2/\text{Si}$ memristive cells, a comparison of the I-V characteristics of a cell with different stoichiometry (x) of Li_xCoO_2 was made. The Li content modification was achieved through a chemical delithiation process as described in the experimental section. I-V sweeps were performed on the same cells ($500 \times 500 \mu\text{m}^2$) before and after chemical delithiation. Chemical affinity of loosely bound Li^+ ions to the acidic solution leads to the deintercalation and diffusion of Li^+ ions from the laminar Li_xCoO_2 structure toward the main solution.

Temporal monitoring of the removal of Li^+ ions from the structure was undertaken through GIXRD analysis of the chemically treated thin film for various infusion durations. Fig. 3 shows the shift of the (003) Li_xCoO_2 peak with increasing (total) infusion time, which indicates a modification of the c-axis lattice parameter. Fig. 4 shows the correlation of infusion time with the gradual enlargement of the c-axis lattice parameter in the film (left side), due to the increasing electrostatic repulsion between the CoO_2 layers, and the Li content value (right side).¹⁶ It is apparent that Li^+ ions are gradually removed from the octahedral sites between the CoO_2 layers resulting in the formation of a Li-deficient Li_xCoO_2 thin film. The chemical delithiation process was terminated when the Li

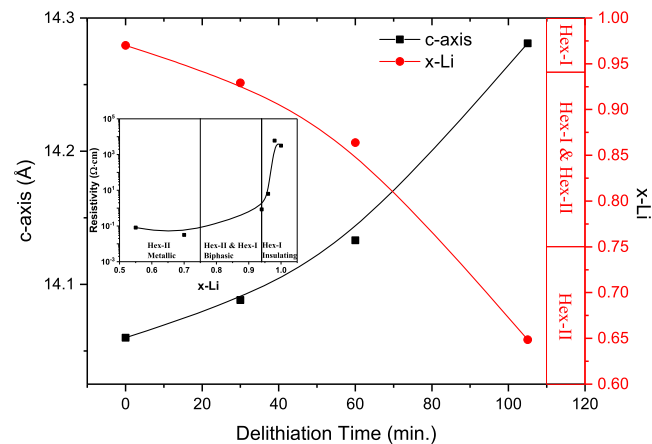


FIG. 4. c-axis lattice parameter (left, black squares) and Li content (right, red circles) of a Li_xCoO_2 layer as a function of delithiation time. Inset shows the dependence of Li_xCoO_2 resistivity on Li content. Data of the inset plot are extracted from Ref. 16.

content reached $x \sim 0.65$ ensuring that Li_xCoO_2 was in the metallic Hex-II phase, as is evident from the dependence of Li_xCoO_2 resistivity on the Li content shown in the inset of Fig. 4.¹⁶

Fig. 1 shows the corresponding J-V sweeps for the same $\text{Au}/\text{Li}_x\text{CoO}_2/\text{SiO}_2/\text{Si}$ cell before and after chemical delithiation. The cell before delithiation ($x \sim 0.97$) shows RS behavior, as discussed previously, whereas the same cell following delithiation ($x \sim 0.65$) displays no hysteretic behavior, indicating that no RS takes place. It can therefore be deduced that in order to observe RS phenomena in this type of cells, the Li_xCoO_2 films must be initially in the insulating Hex-I phase, which requires the initial Li content of the film to be $x > 0.93$. Hence, this is the first time direct proof is provided concerning the critical relation of Li stoichiometry to the RS mechanism, and is indicative of the underlying mechanism being the metal-to-insulator transition of the Li_xCoO_2 film. Additionally, these results indicate that Li-ion intercalation/deintercalation originating from the active Li_xCoO_2 layer plays the dominant role in RS and no contribution is made to RS from the other constituent layers of the memristive cells, apart from the bottom Si electrode, which acts as the host of the Li^+ ions according to the proposed mechanism. It is noted that a similar cell structure albeit with $x \sim 0.7$ (i.e., Li_xCoO_2 in the metallic phase) has been investigated as a potential thin film solid-state source of electric power and no RS behavior has been reported to occur.^{22,23} In this configuration, the Si substrate functions as the anode, the Li_xCoO_2 thin film functions as the cathode, and the SiO_2 layer functions as the solid electrolyte.

The similarity of the aforementioned proposed mechanism to battery cycling and the lack of necessity for an electroforming step have led to the speculation that the RS switching is not of filamentary nature. To determine whether the nature of RS is homogeneous or filamentary, the dependence of I_{on} (measured current at LRS) and I_{off} (measured current at HRS) on the surface area of the top Au electrode was investigated (a schematic diagram of the investigated cells is shown in the inset of Fig. 5). Filamentary switching should result in a very low (or no) correlation²⁴ of electrode area with I_{on} or I_{off} . Conversely, homogeneous switching, which is a bulk effect, is expected to exhibit a direct correlation between electrode area and I_{on} and I_{off} .

Fig. 5 is a log-log plot of I_{on} and I_{off} currents as a function of Au electrode area. A quasi linear dependence of $\log(I_{\text{on}})$ and $\log(I_{\text{off}})$ on the logarithm of the top electrode area is observed with positive slopes of ~ 0.6 for both measured resistance states. The difference of almost three orders of magnitude between the HRS and LRS current levels is attributed to the modification in the resistivity of Li_xCoO_2

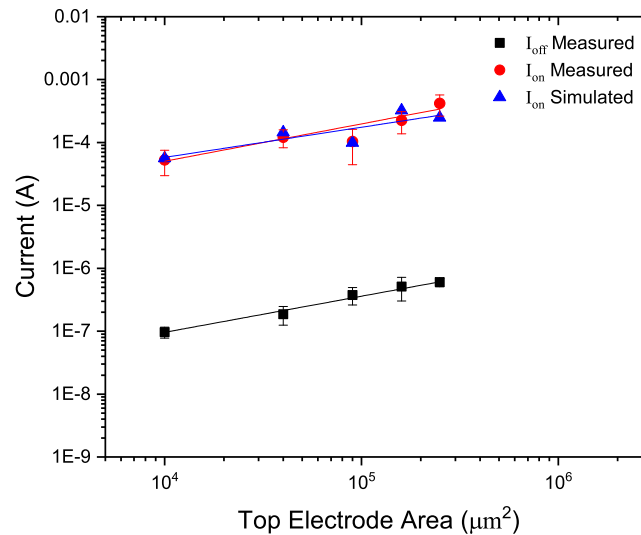


FIG. 5. Dependence of current on top electrode area of $\text{Au}/\text{Li}_x\text{CoO}_2/\text{SiO}_2/\text{Si}$ memristive cells: experimental I_{off} (at -2 V; black squares), experimental I_{on} (at -2 V; red circles) and simulated I_{on} (at -2 V; blue triangles). Inset: a cross-section schematic diagram of five cells defined by the Au (yellow) top electrodes of 500×500 , 400×400 , 300×300 , 200×200 and $100 \times 100 \mu\text{m}^2$, as deposited on a Li_xCoO_2 thin film (blue) grown on a Si (grey)/native SiO_2 (black) substrate. The x and y dimensions are not to scale.

layer upon its switching from insulating to metallic phase, as discussed above and shown in the inset of Fig. 4. These results entrench the hypothesis of a homogeneous mechanism for Au/Li_xCoO₂/SiO₂/Si thin film memristive cells.

Simulation studies on the same cell configuration were carried out in order to corroborate the experimental results discussed above. For the simulation, specific resistivity value has been assigned to the Li_xCoO₂ layer corresponding to LRS,¹⁶ typical literature resistivity values have been used for the rest of the cell constituent layers, and a homogeneous effect is inherently adopted. A comparison of the experimental with the simulated data indicates that a quasi linear dependence of log(I_{on}) on the logarithm of the top electrode area is observed. Additionally, the current levels are similar in both experimental and simulated LRS states. Therefore, the simulation results provide additional support for the proposed homogeneous nature of RS in Au/Li_xCoO₂/SiO₂/Si thin film memristive cells.

This work reports on the results of a new series of experiments concerning two important aspects of the proposed RS mechanism in Au/Li_xCoO₂/SiO₂/Si memristive cells: (i) the microscopic origin and (ii) the nature of the underlying RS mechanism. The microscopic origin of the RS mechanism is shown through chemical delithiation experiments to be the metal-to-insulator transition in the active Li_xCoO₂ layer. The underlying RS mechanism is shown – through experimental and simulation studies of the current dependence on the top electrode area – to be of a homogeneous nature.

C. M. O. gratefully acknowledges financial support from the Graduate School at the University of Cyprus through the program of Ph.D. student fellowships. In addition, the authors thank Prof. T. Stylianopoulos and Mr. F. Kakoutsis for giving access to their computer facilities.

- ¹ T. W. Hickmott, *J. Appl. Phys.* **33**, 2669 (1962).
- ² R. Waser and M. Aono, *Nat. Mater.* **6**, 833 (2007).
- ³ R. Waser, R. Dittmann, G. Staikov, and K. Szot, *Adv. Mater.* **21**, 2632 (2009).
- ⁴ D. Ielmini, R. Bruchhaus, and R. Waser, *Phase Transitions* **84**, 570 (2011).
- ⁵ D. Ielmini, *Semicond. Sci. Technol.* **31**, 063002 (2016).
- ⁶ I. Valov, R. Waser, J. R. Jameson, and M. N. Kozicki, *Nanotechnology* **22**, 254003 (2011).
- ⁷ S. Tappertzhofen, I. Valov, T. Tsuruoka, T. Hasegawa, R. Waser, and M. Aono, *ACS Nano* **7**, 6396 (2013).
- ⁸ G. S. Snider, in *IEEE Int. Symp. on Nanoscale Architectures* (June 2008), Anaheim, USA.
- ⁹ I. Valov, E. Linn, S. Tappertzhofen, S. Schmelzer, J. van den Hurk, F. Lentz, and R. Waser, *Nat. Commun.* **4**, 1771 (2013).
- ¹⁰ R. Dittmann, R. Muenstermann, I. Krug, D. Park, T. Menke, J. Mayer, A. Besmehn, F. Kronast, C. M. Schneider, and R. Waser, *Proc. IEEE* **100**, 1979 (2012).
- ¹¹ A. T. Kutbee, M. T. Ghoneim, S. M. Ahmad, and M. M. Hussain, *IEEE Trans. Nanotechnol.* **15**(3), 402 (2016).
- ¹² A. Moradpour, O. Schneegans, S. Franger, A. Revcolevschi, R. Salot, P. Auban-Senzier, C. Pasquier, E. Svoukis, J. Giapintzakis, O. Dragos, V. Ciomaga, L. Pinsard-Gaudart, and P. Chrétien, *Adv. Mater.* **23**, 4141 (2011).
- ¹³ V. H. Mai, A. Moradpour, P. Auban Senzier, C. Pasquier, K. Wang, M. J. Rozenberg, J. Giapintzakis, C. N. Mihailescu, C. M. Orfanidou, E. Svoukis, A. Breza, Ch. B. Lioutas, S. Franger, A. Revcolevschi, T. Maroutian, P. Lecoeur, P. Aubert, G. Agnus, R. Salot, P. A. Albouy, R. Weil, D. Alamarguy, K. March, F. Jomard, P. Chrétien, and O. Schneegans, *Sci. Rep.* **5**, 7761 (2015).
- ¹⁴ V. S. Nguyen, V. H. Mai, P. Auban Senzier, C. Pasquier, K. Wang, M. J. Rozenberg, N. Brun, K. March, F. Jomard, J. Giapintzakis, C. N. Mihailescu, E. Kyriakides, P. Nukala, T. Maroutian, G. Agnus, P. Lecoeur, S. Matzen, P. Aubert, S. Franger, R. Salot, P. A. Albouy, D. Alamarguy, B. Dkhil, P. Chrétien, and O. Schneegans, *Small* **14**, 1801038 (2018).
- ¹⁵ Y. Ishida, A. Mizutani, K. Sugiura, H. Ohta, and K. Koumoto, *Phys. Rev. B* **82**, 075325 (2010).
- ¹⁶ M. Ménétrier, I. Saadoun, S. Levasseur, and C. Delmas, *J. Mater. Chem.* **9**, 1135 (1999).
- ¹⁷ L. Dahéron, R. Dedyvère, H. Martinez, M. Ménétrier, C. Denage, C. Delmas, and D. Gonbeau, *Chem. Mater.* **20**, 583 (2008).
- ¹⁸ M. Shibuya, T. Nishina, T. Matsue, and I. Uchida, *J. Electrochem. Soc.* **143**, 3157 (1996).
- ¹⁹ J. Molenda, A. Stoklosa, and T. Bak, *Solid State Ionics* **36**, 53 (1989).
- ²⁰ J. T. Hertz, Q. Huang, T. McQueen, T. Klimczuk, J. W. G. Bos, L. Viciu, and R. J. Cava, *Phys. Rev. B* **77**, 075119 (2008).
- ²¹ K. Hoang and M. D. Johannes, *J. Mater. Chem. A* **2**, 5224 (2014).
- ²² N. Ariel, G. Ceder, D. R. Sadoway, and E. Fitzgerald, *J. Appl. Phys.* **98**, 023516 (2005).
- ²³ N. Ariel, D. M. Isaacson, and E. Fitzgerald, *J. Vac. Sci. Technol. B* **24**, 562 (2006).
- ²⁴ H. Sim, H. Choi, D. Lee, M. Chang, D. Choi, Y. Son, E. H. Lee, W. Kim, Y. Park, I. K. Yoo, and H. Hwang, *IEEE Int. Electron Devices Meet., Tech. Dig.* **2005**, 758.